Structure and Nonlinear Optical Properties of Cationic Defects in Amorphous Silicon Dioxide. 1. Cluster Studies†

Antonio M. Ferreira* and Henry A. Kurtz

Department of Chemistry and Computational Research on Materials Institute, University of Memphis, Memphis, Tennessee 38152

Shashi P. Karna

Air Force Research Laboratory, Space Vehicles Directorate, 3550 Aberdeen Avenue, SE Kirtland AFB, New Mexico 87117-5776

Received: October 27, 1999; In Final Form: March 13, 2000

We present the first systematic ab initio study of cationic defects in *a*-SiO_2. Cluster models are employed to show that the presence of cationic defects (H^+, Li^+, Be^{2+}, Na^+, and Mg^{2+}) can have large effects on both the structure and (hyper)polarizabilities of the material. The interaction of the proton with the cluster model demonstrates that it is unique compared to the other group IA and IIA cations in the study.

Introduction

An important experiment on optical fibers was performed in 1986 by Österberg and Margulis in which second harmonic generation occurred in a fused silica optical fiber.[1] After several hours of irradiation with 1064 nm light, a weak second harmonic generation (SHG) signal appeared in the visible region (532 nm) with 3% optical power conversion. This is particularly noteworthy since *a*-SiO_2 is a continuous random network[2] (CRN) in which there should be no net dipole moment and thus no second-order optical response. It has been found that this optical response can be induced by seeding the fiber with a 532 nm source before irradiation with the 1064 nm light.[3] In this case the SHG signal was induced with the same optical power conversion in a matter of minutes. The changes induced by using a seed laser have been shown to be temporary, and subsequent irradiation at 1064 nm in the absence of the seed laser showed no improvement in SHG response time when carried out 12 h after the initial experiment. Recently, SHG of infrared (IR) light has also been observed in dc electric field poled fused silica,[4] thin SiO_2 film,[5] and in ultraviolet (UV) light poled germanium-doped silica fibers.[6]

The observation of such phenomena from a CRN material raises important fundamental questions about the optical response in these fibers. Several mechanisms have been proposed[7−11] for this process, though the mechanism of the SHG generation in such optical fibers is not understood. It is interesting to note that the proposed mechanisms for SHG in silica-based materials range from a purely microscopic effect[8] caused by point defects in the materials to a purely bulk effect induced by a dc electric field created by the generation and transport of charged species.[7,9,10] Yet another mechanism, recently proposed to explain SHG in UV poled Ge-doped silica, involves a combination of microscopic and bulk effects caused by the alignment of local fields created by charged native point defects.[11] In view of the potential technological applications of nonlinear optical (NLO) effects in silica-based materials and a complete lack of fundamental knowledge about their origin, we have performed ab initio time-dependent Hartree−Fock (TDHF) calculations on model clusters representing local atomic arrangements in silica in the presence of various charged species that have been detected in amorphous SiO_2.[12]

In this paper we present the results of our study of the effect on the local geometry and microscopic nonlinear optical properties of the oxide network in the presence of positively charged ions. While neutral point defects, such as the 3-fold coordinated Si/Ge atom, peroxy linkage, and atomic H[13,14] also constitute the family of point defects found in amorphous silica, it is generally believed that the SHG in these materials involves space charge field created by positively charged species.[9−11] Furthermore, in a previous ab initio TDHF calculation it was shown that the presence of a proton (H^+) around a SiO_2 cluster in oxide network substantially changes the value of the second-order NLO coefficient.[15] Therefore, the current study focuses on the effect of several positively charged species, H^+, Li^+, Be^{2+}, Na^+, and Mg^{2+}, on the structure and microscopic NLO properties of the oxide network.

Computational Methods

Modeling bulk materials, such as *a*-SiO_2, is a computationally intensive endeavor and there are various approaches that can be employed to address the problem. For the present study, we have chosen to use model clusters to evaluate the structural and optical changes induced by various potential cationic defects. In the present study, we chose to work with a Si_2O_7 (Figure 1a) cluster to represent the local structure of a regular oxide network. Hydrogen atoms terminate the valencies of the outer six O atoms. Most of the essential features of a regular *a*-SiO_2 network are represented by this cluster. Furthermore, the selection of a moderate-size cluster, such as the Si_2O_7, allowed us to systematically improve the basis set to the current limit of the computational resources.

Calculations were carried out with the GAMESS[16] ab initio computational chemistry software. Geometry optimizations were performed at the ab initio restricted Hartree−Fock (RHF) level

† Part of the special issue "Electronic and Nonlinear Optical Materials: Theory and Modeling".

10.1021/jp993802t CCC: $19.00
Published on Web 04/20/2000

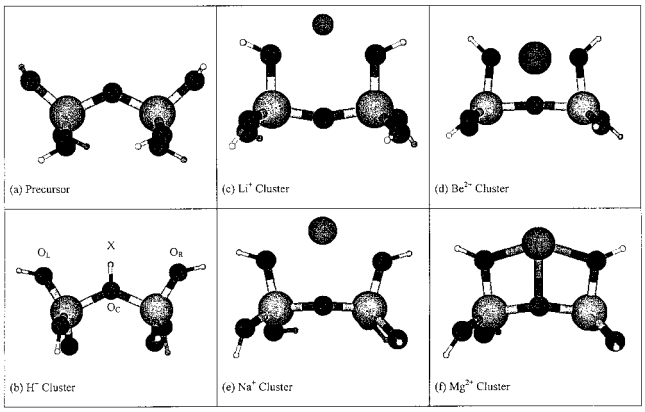

Figure 1. Calculated geometries for the precursor (a), H^+ (b), Li^+ (c), Be^{2+} (d), Na^+ (e), and Mg^{2+} (f) cationic clusters at the RHF level with the 6-31G** basis set.

TABLE 1: Calculated O−X Bond Distance and Bond Angles at Optimized Equilibrium Geometry in Cationic Oxide Cluster

	distance (Å)		angles (deg)	
X	$X-O_C$	$X-O_{L/R}$	$O_C-Si-O_{L/R}$	$Si-O_C-Si$
precursor			113	131
H^+	0.94	2.27	105	131
Li^+	2.90	1.88	101	160
Na^+	2.51	2.30	98	167
Be^{2+}	1.64	1.55	82	173
Mg^{2+}	2.07	1.97	89	148

of theory using a 6-31G** basis set.[17] The NLO properties were calculated using the TDHF method[18] according to the Karna and Dupuis formulation.[19] Frequency-dependent results were obtained at a fundamental frequency of the Nd:YAG laser (λ = 1064 nm).

Structure

The fully optimized RHF/6-31G** geometries for the cationic clusters are shown in Figure 1 and can be classified in two general categories based on the interaction of the ion with the cluster. Table 1 contains some of the geometric data for each species, with the atom labels corresponding to the scheme used in Figure 1b. X represents one of the cationic species listed in the table and, therefore, the cluster has a net charge of either +1 or +2. It is also important to note that O_L and O_R are equivalent positions even though the cluster as a whole possesses no symmetry.

From the structural data we see that the proton behaves in a clearly different manner from the other cations used in the present study. Based solely on the bond length information, we see that the proton is bound much more closely than the other cations and that it binds directly to a single oxygen atom, consistent with the formation of a covalent bond. Conversely, the other cations in the study interact with multiple oxygens in the cluster in a mostly electrostatic manner. Also, the proton creates the smallest distortions of the cluster from the precursor geometry. The general trend is toward larger distortions of the $O_C-Si-O_{L/R}$ angle as atomic number increases. Increasing the charge within a period leads to shorter distances from the central oxygen atom (O_C) and larger distortions are created in the cluster in order to accommodate the cation. Similarly, as the size of the cations increase from the second to the third period, so does the magnitude of the distortion in the angles around O_C. A particular feature of the larger ions (Na^+ and Mg^{2+}) is a distortion from planarity when viewed along the $X-O_C$ axis.

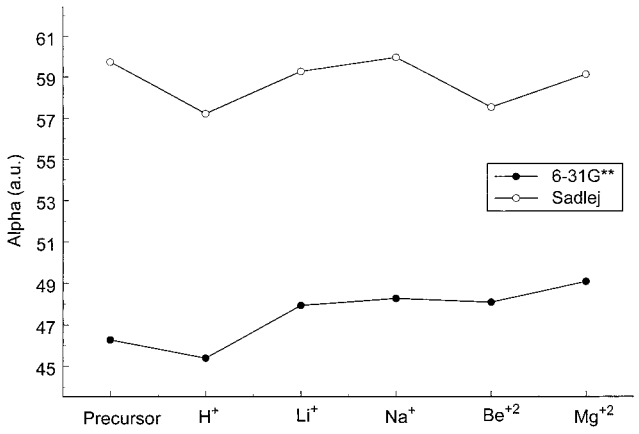

Figure 2. Static polarizabilities (α) for precursor cluster (P) and cation complexes (P−X) with both 6-31G** and Sadlej basis sets.

TABLE 2: Calculated Binding Energy of Cationic Species in *a*-SiO_2.

	H^+	Li^+	Na^+	Be^{2+}	Mg^{2+}
au	0.322017	0.104383	0.075087	0.488452	0.288210
eV	8.76	2.84	2.04	13.29	7.84

These clusters are distorted from a linear $O_L-O_C-O_R$ arrangement to 137° in both cases.

The Be^{2+} ion is a particularly interesting case. It follows the general trends outlined above, but creates the largest distortions from the unperturbed cluster. Its small size allows a short $Be^{2+}-O_C$ bond very similar to that of the proton, but the +2 charge causes strong interactions with the O_L and O_R oxygens, creating much larger distortions.

We see evidence that the coordination number for these cations is increasing with atomic number as expected. As previously mentioned, the proton is interacting directly with only one of the oxygen atoms. In contrast, the lithium cation is bound more strongly to two of the oxygens, and beryllium, sodium, and magnesium are each interacting directly with all three of the central oxygen atoms. It is expected that this trend in coordination will become more pronounced in the ring systems proposed below.

The energetics for the cationic systems also shows a distinct difference between the proton and the other cations in the study. We can see from the information in Table 2 that the proton has 4 times the binding energy of the other group IA cations and is competitive with the binding energies of the group IIA cations. Only the Be^{2+} cation, with the advantages of small size and high charge, binds more strongly, but the large distortions in the geometry can be used to explain this behavior. Binding energies for the other cations tend to decrease with increasing size and increase with charge as expected. Again, this points to the covalent versus electrostatic interactions that differentiate the proton from the other cations.

NLO Properties

The initial cluster with no cation present will be referred to as the "precursor" in the following discussion. The results of the TDHF calculations for the precursor and cationic clusters are given in Table 3. NLO properties are known to be sensitive to basis set quality so properties were obtained with the standard 6-31G** basis as well as the much larger Sadlej[20,21] basis, designed for polarizability calculations. Figures 2−4 illustrate the relative values for α, β, and γ for the clusters as well as the effects of basis set. For the precursor, the calculated polarizability (α) increases by nearly 30% in going from the 6-31G**

TABLE 3: Calculated Dipole Moment, μ, and (Hyper)polarizablities (α, β, γ)[a,b]

	precursor		P−H$^+$		P−Li$^+$		P−Na$^+$		P−Be^{2+}		P−Mg^{2+}	
	6-31G**	Sadlej	6-31G**	Sadlej	6-31G**	Sadlej	6-31G**	Sadlej	6-31G**	Sadlej	6-31G**	Sadlej
$\lvert\mu\rvert$	1.0495	0.8799	0.1224	0.2053	5.0568	5.2004	5.9702	6.0047	4.9242	4.8738	8.4144	8.3181
$\langle\alpha(0)\rangle$	46.2749	59.7372	45.3927	57.2167	47.9327	59.2682	48.2651	59.9697	48.0858	57.5254	49.0756	59.1107
$\langle\alpha(\omega)\rangle$	46.4682	60.0181	45.5637	57.4477	48.1241	59.5167	48.4573	60.2195	48.2699	57.7528	49.2753	59.3553
$\beta_{\|\|}(0)$	41.47	28.93	21.56	7.29	199.61	106.90	238.82	108.47	181.14	123.85	387.99	269.98
$\beta_{\|\|}$SHG	43.01	30.52	22.13	7.36	209.72	113.49	251.55	115.86	189.36	130.46	410.38	288.13
$\beta_{\|\|}$OR	41.97	29.45	21.74	7.31	202.88	109.03	242.94	110.86	183.81	125.99	395.22	275.83
$\beta_{\|\|}$EOPE	41.97	29.45	21.74	7.31	202.88	109.03	242.94	110.86	183.81	125.99	395.22	275.83
$\langle\gamma(0)\rangle$	1989.2	4708.4	1879.8	3471.6	2647.4	4049.2	2829.1	4181.5	2088.7	3012.9	2888.0	3701.6
$\langle\gamma^{\mathrm{THG}}\rangle$	2227.4	5448.4	2085.9	3896.3	2972.3	4579.1	3186.2	4739.1	2320.2	3348.9	3291.7	4197.0
$\langle\gamma^{\mathrm{EFISHG}}\rangle$	2103.1	5057.3	1978.7	3674.4	2802.5	4301.5	2999.3	4446.7	2199.8	3174.1	3079.1	3936.9
$\langle\gamma^{\mathrm{IDRI}}\rangle$	2064.1	4936.8	1944.9	3604.8	2749.3	4214.9	2940.8	4355.6	2161.8	3119.0	3013.4	3856.0
$\langle\gamma^{\mathrm{OKE}}\rangle$	2026.1	4820.4	1911.9	3537.2	2697.5	4130.7	2884.1	4267.1	2124.7	3065.2	2949.5	3777.4

[a] All α, β, and γ values are in atomic units and μ is in debyes. [b] For α 1 au = 1.4819×10^{-25} esu, for β 1 au = $8.629\,11 \times 10^{-33}$ esu, and for γ 1 au = $5.036\,70 \times 10^{-40}$ esu.

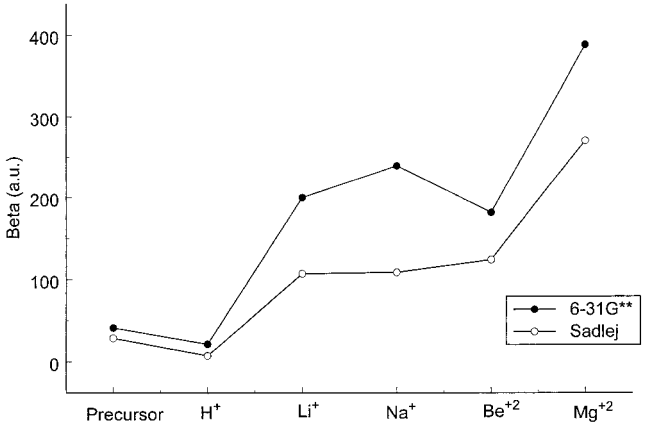

Figure 3. Static first hyperpolarizabilities (β) for precursor cluster (P) and cation complexes (P−X) with both 6-31G** and Sadlej basis sets.

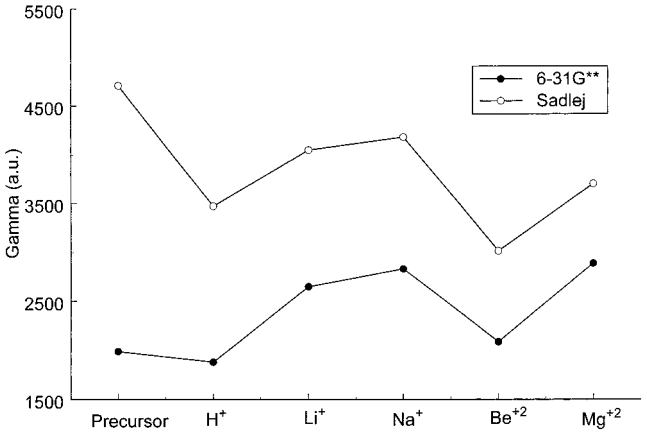

Figure 4. Static second hyperpolarizabilities (γ) for precursor cluster (P) and Cation complexes (P−X) with both 6-31G** and Sadlej basis sets.

basis to the Sadlej basis. For the second hyperpolarizabilities (γ) this increase is nearly 140% while the first hyperpolarizability (β) shows a 30% *decrease*. The basis set effect for the optimized cation clusters is similar to those in the precursor cluster. The polarizability (α) increases 26% for the H^+ cluster, 24% for the Li^+ and Na^+ clusters, and 20% for the Be^{2+} and Mg^{2+} clusters. The second hyperpolarizabilities (γ) increase by 85, 53, 44, 48, and 28% for H^+, Li^+, Be^{2+}, Na^+, and Mg^{2+}, respectively. Like the precursor, the better basis set results in a decrease in the first hyperpolarizabilities of −66, −46, −32, −55, and −30%, for H^+, Li^+, Be^{2+}, Na^+, and Mg^{2+}, respectively. While the 6-31G** basis set does not provide good quantitative results, the figures show that this basis set seems to yield good relative results which should allow calculations on much larger clusters.

TABLE 4: Calculated (Hyper)polarizablities in Distorted SiO_2 Complex at Cation Cluster Geometry

	basis set	$\lvert\mu\rvert$	$\langle\alpha(0)\rangle$	$\beta_{\|\|}(0)$	$\langle\gamma(0)\rangle$
H^+	6-31G**	3.7275	47.6129	168.14	2500.2
	Sadlej	3.3192	61.5920	129.23	5663.2
Li^+	6-31G**	3.9087	46.7771	208.40	2169.6
	Sadlej	3.5823	60.8678	113.03	5050.5
Na^+	6-31G**	4.1625	46.7888	187.96	2149.0
	Sadlej	3.7735	60.5807	101.68	4983.1
Be^{2+}	6-31G**	4.5183	49.6858	313.57	3113.9
	Sadlej	4.2933	64.2380	191.79	6481.2
Mg^{2+}	6-31G**	5.4204	48.3301	304.13	2561.5
	Sadlej	5.0350	62.5424	177.49	5637.4

[a] All α, β, and γ values are in atomic units and μ is in debyes. Conversion factors are listed in Table 1.

TABLE 5: Property Change from Geometry Distortion Alone with Percentage Change Shown in Parentheses[a]

	basis set	$\lvert\mu\rvert$	$\langle\alpha(0)\rangle$	$\beta_{\|\|}(0)$	$\langle\gamma(0)\rangle$
H^+	6-31G**	2.6781 (255)	1.3380 (3)	126.67 (305)	511.0 (26)
	Sadlej	2.4393 (277)	1.8548 (3)	100.30 (347)	954.8 (20)
Li^+	6-31G**	2.8592 (272)	0.5022 (1)	166.93 (403)	180.4 (9)
	Sadlej	2.7024 (307)	1.1306 (2)	84.10 (291)	342.0 (7)
Na^+	6-31G**	3.1130 (297)	0.5139 (1)	146.49 (353)	159.8 (8)
	Sadlej	2.8936 (329)	0.8435 (1)	72.75 (251)	274.7 (6)
Be^{2+}	6-31G**	3.4688 (331)	3.4109 (7)	272.10 (656)	1124.6 (57)
	Sadlej	3.4134 (388)	4.5008 (8)	162.86 (563)	1772.8 (38)
Mg^{2+}	6-31G**	4.3709 (416)	2.0552 (4)	262.67 (633)	572.3 (29)
	Sadlej	4.1551 (472)	2.7952 (5)	148.55 (513)	929.0 (20)

[a] All α, β, and γ values are in atomic units and μ is in debyes.

The current model allows large distortions in geometry in these small cluster systems, as evidenced by the Be^{2+}, Na^+, and Mg^{2+} results. It is possible to separate the contribution leading to differences in the optical response induced by the cation into contributions due to the large change in local geometry of the SiO_2 unit and the electronic effects induced by the presence of the cation in the complex. In order to understand the role the geometric changes alone play in modifying in (hyper)polarizabilities of the cluster systems, the optical properties of the distorted clusters without the ion present were calculated and are presented in Table 4. The distorted cluster is defined as the original precursor cluster in the geometry of the cation cluster, without the cation. The property differences between distorted clusters and the original precursor are found in Table 5. A particularly interesting trend is that of the first hyperpolarizability, which is very sensitive to geometry changes

TABLE 6: Cation (Hyper)polarizablities Results[a]

	Li^+		Na^+		Be^{2+}		Mg^{2+}	
	6-31G**	Sadlej	6-31G**	Sadlej	6-31G**	Sadlej	6-31G**	Sadlej
$\langle\alpha(0)\rangle$	0.0582	0.0555	0.3458	0.8126	0.0240	0.0119	0.1290	0.4222
$\langle\alpha(\omega)\rangle$	0.0582	0.0555	0.3460	0.8129	0.0240	0.0120	0.1291	0.4222
$\langle\gamma(0)\rangle$	0.6498	0.8371	5.8664	2.2094	0.0225	0.0367	0.5215	0.3172
$\langle\gamma^{THG}\rangle$	0.6527	0.8409	5.9418	2.2448	0.0225	0.0367	0.5244	0.3193
$\langle\gamma^{EFISHG}\rangle$	0.6512	0.8390	5.9040	2.2270	0.0225	0.0367	0.5230	0.3183
$\langle\gamma^{IDRI}\rangle$	0.6507	0.8383	5.8914	2.2211	0.0225	0.0367	0.5225	0.3179
$\langle\gamma^{OKE}\rangle$	0.6502	0.8377	5.8789	2.2152	0.0225	0.0367	0.5220	0.3176

[a] All α, β, and γ values are in atomic units and μ is in debyes.

TABLE 7: Interaction Values[a] for the Interaction of the SiO_2 Unit with the Cation and Percentage of Total Value (in Parentheses)

	$\langle\alpha(0)\rangle$	$\beta_{\|\|}(0)$	$\langle\gamma(0)\rangle$	energy[b]
H^+	−4.3753 (−8)	−121.94 (−1673)	−2191.6 (−63)	211.10
Li^+	−1.6551 (−3)	−6.13 (−6)	−1002.1 (−25)	73.65
Na^+	−1.4236 (−2)	−6.79 (−6)	−803.8 (−19)	50.87
Be^{2+}	−6.7245 (−2)	−67.94 (−55)	−3468.3 (−115)	373.81
Mg^{2+}	−3.8439 (−7)	92.50 (+34)	−1936.2 9−52)	216.88

[a] All α, β, and γ values are in atomic units, μ is in debyes, and energy is in kcal/mol.

and shows an increase of 291%−656% attributed solely to the geometric distortion of the cluster. We note that the changes in geometry also induce increases in the dipole moments ranging from 255% to 416%, which accounts for the dramatic increase in hyperpolarizabilities. The +2 clusters had the largest distortions in geometry and the largest changes in the optical response. For these clusters, the second hyperpolarizability changes are nearly an order of magnitude larger than those for the other cation clusters and change by 20%−40% from those for the precursor while the increase is only 6%−7% for the +1 cations and roughly 27% for H^+. The geometry changes also caused an increase in polarizabilities for all of the clusters ranging from 1% to 7.5%. Again, the changes for the +2 clusters are much larger than the +1 clusters.

We can also examine the interaction of the cations with the SiO_2-like cluster by looking at the interaction properties, defined as $P_{interaction} = P_{cluster} - (P_{distorted\ cluster} + P_{cation})$.[22] For example, the change in polarizability value due to the electronic interaction of the SiO_2 cluster and the cation is given by $\Delta\alpha = \alpha_{interaction} = \alpha_{cluster} - (\alpha_{distorted\ cluster} + \alpha_{cation})$. In order to compute these interaction properties, the bare cation properties have been computed and are given in Table 6.

Basis set quality is an important consideration in evaluating interaction properties. For example, for the Li^+ cluster $\Delta\alpha$(6-31G**) is 1.0974 and $\Delta\alpha$(Sadlej) is −1.6551: they have completely different signs! An additional complication for computing interaction properties in this manner is the effect of basis set superposition errors (BSSE). When BSSE is taken into account by using the entire basis set for each fragment calculation, the Li^+ cluster results become $\Delta\alpha$(6-31G**) = −0.064 53 and $\Delta\alpha$(Sadlej) = −1.7520, with the signs now in agreement. This also shows that the 6-31G** basis set has large BSSE effects, while the more complete Sadlej basis exhibits small BSSE effects. Therefore, only the interaction values for the (hyper)polarizabilities and the energies (binding energies) based on the Sadlej basis set results will be presented (Table 7).

The (hyper)polarizability values for the cations (Table 6) are all very small compared to the cluster values and thus do not contribute a significant amount to the interaction values. The interaction effects on the polarizabilities are all negative but fairly small (2%−3%), except for the covalently bound H^+ and the large, highly charged Mg^{2+} ion. The interaction effects for the second hyperpolarizabilities are also all negative. A simple interpretation is that the presence of the +2 charge strongly attracts the electrons, making them less polarizable. The presence of the charge has a much larger effect on the interaction first hyperpolarizability. An interesting result of our present calculations is that for the Mg^{2+} ion cluster, $\Delta\beta$ is positive. Even from the other $\Delta\beta$ results it is not possible to give a simple interpretation, except to note that the effect is small for the +1 ions and large for the +2 ions. The very large value for the covalent H^+ system shows that it is very different from the other ionic systems.

Summary

There are several important conclusions one can draw from this work. The present study provides clear evidence that the cluster model is appropriate for describing the local distortions that give rise to very large changes in (hyper)polarizability values. Because the CRN of *a*-SiO_2 is extremely flexible, we feel that predictions based on large local distortions of the small clusters presented here will be adequate for qualitative descriptions of the effects for these cationic species.

One important improvement needed involves testing if the cluster model is truly appropriate for these systems. Large distortions, such as those exhibited in the Be^{2+} cluster, may not be a physically accurate picture. The flexibility afforded a small cluster may be too great to give an accurate picture of defect sites in the bulk material. In order to correct these difficulties, theoretical studies of larger ring systems ($Si_6O_6H_{12}$) are currently underway. Preliminary results from these calculations indicate that the local distortions of the small clusters should not be a cause for concern. Another important set of structures would be cagelike systems. Calculations are underway on larger cluster systems, such as a 106-atom SiO_2 cluster, to further examine the validity of these small cluster models.

Second, we see more evidence that protons in *a*-SiO_2 behave very differently from other cations of similar size and charge, consistent with the different type of bonding in this case. In each case, the properties of the proton-related cluster contrast with the trends seen in the other cations. In addition to the optical properties of these defects, the structural information is equally important to the development of MOS technology. Understanding the microscopic structure of defects involving cationic species is an important step in understanding how to manipulate the role these defects play in high-quality electronic materials. It is hoped that future studies of this type will yield greater insight into defect mechanisms and their properties for use in materials design.

This points to an area of materials design for which theory is particularly well suited. It is now possible to study the nonlinear optical properties of transition metals using compu-

tational methods that avoid the all-electron problem[23] to aid in the screening and identification of optical materials. Using these methods, we can investigate the properties of other cationic species for evaluation as potential dopants to be employed in novel electronic and optical materials.

Acknowledgment. H.A.K. and A.M.F. acknowledge the support of the NSF for the computational chemistry program at the University of Memphis through grants STI-9602656 (Academic Research Infrastructure Program) and CHE-9708517 (Chemical Research Instrumentation and Facilities Program).

References and Notes

(1) Österberg, U.; Margulis, W. *Opt. Lett.* **1986**, *11*, 516.

(2) Zachareisen, W. H. *J. Am. Chem. Soc.* **1932**, *54*, 3841.

(3) Stolen, R. H.; Tom, H. W. K. *Opt. Lett.* **1987**, *12*, 585.

(4) Myers, R. A.; Mukherjee, N.; Brueck, S. R. J. *Opt. Lett.* **1991**, *16*, 1732.

(5) Kester, J. J.; Wolf, P. W.; White, W. R. *Opt. Lett.* **1992**, *17*, 1779.

(6) Fujiwara, T.; Wong, D.; Zhao, Y.; Fleming, S.; Poole, S.; Sceates M. *Electron. Lett.* **1995**, *31*, 573.

(7) Dominic, V.; Feinberg, J. *Phys. Rev. Lett.* **1993**, *71*, 3446.

(8) Tsai, T. E.; Saifi, M. A.; Frieble, E. J.; Griscom, D. L.; Österberg, U. *Opt. Lett.* **1989**, *14*, 1023.

(9) Le Calvez, A., Freysz, E.; Ducasse, A., *Opt. Lett.* **1997**, *22*, 1547.

(10) Alley, T. G.; Brueck, S. R. J.; Meyers, R. A. *J. Non-Cryst. Solids* **1998**, *242*, 165.

(11) Fujiwara, T.; Takahasi, M.; Ikushima, A. J. *Electron. Lett.* **1997**, *33*, 980.

(12) (a) Poumellec, B.; Fevrier, H.; Gabriagues, J.-M. *Mater. Sci. Eng. B* **1991**, *9*, 449. (b) Becker, K.; Yang, L.; Haglund Jr., R. F.; Magruder, R. H.; Weeks, R. A.; Zuhr, R. A. *Nucl. Instrum. Methods Phys. Res. B* **1991**, *59*, 1304.

(13) Griscom, D. L. *Proc. Mater. Res. Soc.* **1986**, *61*, 213.

(14) Weeks, R. A. *J. Non-Cryst. Solids* **1994**, *179*, 1.

(15) Karna, S. P.; Ferreira, A. M.; Brothers, C. P.; Pugh, R. D.; Singaraju, B. B. K. *Proc. Int. Soc. Opt. Eng.* **1996**, *2811*, 61.

(16) Schmidt, M. W.; Baldridge, K. K.; Boatz, J. A.; Elbert, S. T.; Gordon, M. S.; Jensen, J. H.; Koseki, S.; Matsunaga, N.; Nguyen, K. A.; Su, S. J.; Windus, T. L.; Dupuis, M.; Montgomery, J. A. *J. Comput. Chem.* **1993**, *14*, 1347.

(17) (a) Ditchfield, R.; Hehre, W. J.; Pople, J. A. *J. Chem. Phys.* **1971**, *54*, 724. (b) Dill, J. D.; Pople, J. A. *J. Chem. Phys.* **1975**, *62*, 2921. (c) Binkley, J. S.; Pople, J. A. *J. Chem. Phys.* **1977**, *66*, 879. (d) Gordon, M. S. *Chem. Phys. Lett.* **1980**, *76*, 163. (e) Francl, M. M.; Pietro, W. J.; Hehre, W. J.; Binkley, J. S.; Gordon, M. S.; DeFrees, D. J.; Pople, J. A. *J. Chem. Phys.* **1982**, *77*, 3654.

(18) Sekino, H.; Bartlett, R. J. *J. Chem. Phys.* **1986**, *85*, 976.

(19) Karna, S. P.; Dupuis, M. *J. Comput. Chem.* **1991**, *12*, 487.

(20) (a) Sadlej, A. J. *Collect. Czech. Chem. Commun.* **1988**, *53*, 1995. (b) Sadlej, A. J. *Theor. Chim. Acta* **1992**, *79*, 123.

(21) Data for the Sadlej basis set was obtained from the Extensible Computational Chemistry Environment Basis Set Database, Version 1.0, as developed and distributed by the Molecular Science Computing Facility, Environmental and Molecular Sciences Laboratory, which is part of the Pacific Northwest Laboratory, P.O. Box 999, Richland, WA 99352, and funded by the U.S. Department of Energy. The Pacific Northwest Laboratory is a multiprogram laboratory operated by Battelle Memorial Institue for the U.S. Department of Energy under contract DE-AC06-76RLO 1830. Contact David Feller or Karen Schuchardt for further information.

(22) Chen, S.; Kurtz, H. A. *J. Mol. Struct. (THEOCHEM)* **1996**, *388*, 79.

(23) Cundari, T.; Kurtz, H. A.; Zhou, T. *J. Phys. Chem.* **1998**, *107*, 2962.